




20S Proteasome as a Drug Target in *Trichomonas vaginalis*

 Anthony J. O'Donoghue,^{a,b} Betsaida Bibo-Verdugo,^{b,c} Yukiko Miyamoto,^d Steven C Wang,^{b,e} Justin Z. Yang,^d Douglas E. Zuill,^d Shoun Matsuka,^b Zhenze Jiang,^b Jehad Almaliti,^{f,g} Conor R. Caffrey,^{a,b} William H. Gerwick,^{a,b,f} Lars Eckmann^{a,d}

^aCenter for Discovery and Innovation in Parasitic Diseases, University of California, San Diego, La Jolla, California, USA

^bSkaggs School of Pharmacy and Pharmaceutical Sciences, University of California, San Diego, La Jolla, California, USA

^cSanford Burnham Prebys Medical Discovery Institute, La Jolla, California, USA

^dDepartment of Medicine, University of California, San Diego, La Jolla, California, USA

^eDivision of Biological Sciences, University of California, San Diego, La Jolla, California, USA

^fScripps Institution of Oceanography, University of California, San Diego, La Jolla, California, USA

^gDepartment of Pharmaceutical Sciences, Faculty of Pharmacy, The University of Jordan, Amman, Jordan

ABSTRACT Trichomoniasis is a sexually transmitted disease with hundreds of millions of annual cases worldwide. Approved treatment options are limited to two related nitro-heterocyclic compounds, yet resistance to these drugs is an increasing concern. New antimicrobials against the causative agent, *Trichomonas vaginalis*, are urgently needed. We show here that clinically approved anticancer drugs that inhibit the proteasome, a large protease complex with a critical role in degrading intracellular proteins in eukaryotes, have submicromolar activity against the parasite *in vitro* and on-target activity against the enriched *T. vaginalis* proteasome in cell-free assays. Proteomic analysis confirmed that the parasite has all seven α and seven β subunits of the eukaryotic proteasome although they have only modest sequence identities, ranging from 28 to 52%, relative to the respective human proteasome subunits. A screen of proteasome inhibitors derived from a marine natural product, carmaphycin, revealed one derivative, carmaphycin-17, with greater activity against *T. vaginalis* than the reference drug metronidazole, the ability to overcome metronidazole resistance, and reduced human cytotoxicity compared to that of the anticancer proteasome inhibitors. The increased selectivity of carmaphycin-17 for *T. vaginalis* was related to its >5-fold greater potency against the $\beta 1$ and $\beta 5$ catalytic subunits of the *T. vaginalis* proteasome than against the human proteasome subunits. In a murine model of vaginal trichomonad infection, proteasome inhibitors eliminated or significantly reduced parasite burden upon topical treatment without any apparent adverse effects. Together, these findings validate the proteasome of *T. vaginalis* as a therapeutic target for development of a novel class of trichomonacidal agents.

KEYWORDS *Trichomonas vaginalis*, proteasome, protozoa

Trichomonas vaginalis is the causative agent of the most common, nonviral sexually transmitted global infection, with an estimated incidence of 276 million new cases each year (1, 2). In the United States alone, over 3 million cases are estimated to occur annually, with overall prevalence rates of 1.8 to 3.1% in females and 0.5% in males and even higher rates among African American women (8%) and men (4%) (3, 4). In addition to urogenital infections, trichomoniasis increases the risk of adverse pregnancy outcomes (5, 6) and HIV transmission (7), and 15% of HIV-infected women carry concurrent *T. vaginalis* infections (3). Trichomoniasis also increases the incidence and severity of cervical and prostate cancers (8).

Only two drugs are currently FDA approved for the treatment of trichomoniasis, the

Citation O'Donoghue AJ, Bibo-Verdugo B, Miyamoto Y, Wang SC, Yang JZ, Zuill DE, Matsuka S, Jiang Z, Almaliti J, Caffrey CR, Gerwick WH, Eckmann L. 2019. 20S Proteasome as a drug target in *Trichomonas vaginalis*. *Antimicrob Agents Chemother* 63:e00448-19. <https://doi.org/10.1128/AAC.00448-19>.

Copyright © 2019 American Society for Microbiology. All Rights Reserved.

Address correspondence to Anthony J. O'Donoghue, ajodonoghue@ucsd.edu, or Lars Eckmann, leckmann@ucsd.edu.

Received 1 March 2019

Returned for modification 24 April 2019

Accepted 19 August 2019

Accepted manuscript posted online 26 August 2019

Published 22 October 2019

nitro drugs metronidazole and tinidazole. Both are prodrugs that must be activated to reactive intermediates by reductive processes present in susceptible microbes (9). The intermediates form covalent adducts with DNA and protein targets, but the nature and relative importance of these targets in mediating cell killing are not well understood. Oral administration of either drug leads to clinical and microbiological cure in the majority of cases although treatment failures occur in 1 to 17% of patients (10, 11). A recent survey in the United States found that 4.3% of 538 *T. vaginalis* isolates showed metronidazole resistance (12). Higher oral metronidazole doses can sometimes lead to cure of refractory infections but tend to be poorly tolerated (13). Given the prevalence of *T. vaginalis* infections and the increase in resistance (12, 14), an urgent need exists to develop new antimicrobials against trichomoniasis, particularly agents with new targets and mechanisms of action (15, 16).

Proteasomes are large protease complexes that degrade intracellular proteins in all eukaryotes and several prokaryotes. These multisubunit complexes are formed by two rings of seven β subunits (β_1 to β_7) sandwiched between two rings of seven α subunits (17). Proteins targeted for degradation are first unfolded and then threaded into a barrel-shaped core of the proteasome, where the catalytic subunits, β_1 , β_2 , and β_5 , degrade the proteins into peptides. Each of the catalytic β subunits has a distinct substrate specificity that varies between species (18). Because normal proteasome function is required for cell survival, proteasome inhibitors have been developed as agents against cancer, namely, multiple myeloma, in which degradation of large amounts of misfolded proteins is particularly important for cell survival (19). More recently, proteasome inhibition has been explored as a new strategy for antimicrobial drugs against eukaryotic pathogens, particularly *Plasmodium falciparum*, *Trypanosoma cruzi*, *Leishmania donovani*, and *Babesia divergens* (18, 20–24).

The genome of *T. vaginalis* encodes a number of proteolytic enzymes that play a role in host-microbe interactions (25–27). The parasite, like all eukaryotic cells, also produces proteasome subunits, but their importance for parasite growth and survival is poorly defined. Short-term incubation with a proteasome inhibitor leads to autophagy in *T. vaginalis* under glucose-rich growth conditions (28), suggesting a vital function of the proteasome under specific nutrient conditions. In another trichomonad, *Tritrichomonas foetus*, the proteasome inhibitor lactacystin A inhibits parasite growth (29). Based on these initial observations and data from other parasites, we hypothesized that the proteasome of *T. vaginalis* is a valuable target for the development of a novel class of trichomonacidal agents.

RESULTS

Trichomonacidal activity of proteasome inhibitors. *T. vaginalis* encodes ~440 putative proteases in five major classes that include serine, threonine, cysteine, aspartic acid, and metalloproteases (27, 30). To determine whether any of these protease classes may be suitable as novel targets for trichomonacidal agents, we tested the activity of several class-specific inhibitors, including AEBSF [4-(2-aminoethyl)benzenesulfonyl fluoride; specific for serine proteases], MG132 (threonine), E-64 (cysteine), pepstatin (aspartic acid), and phenanthroline (metalloproteases), against *T. vaginalis* trophozoites in a 24-h growth and survival assay. Only MG132 showed significant activity against the parasite, with a 50% effective concentration (EC_{50}) value of 4.2 μ M, whereas the other four inhibitors had no detectable activity at the highest tested concentration of 20 μ M (Fig. 1A). These data suggest that threonine-specific proteases may be new targets for agents against *T. vaginalis*.

Threonine proteases, such as those in the proteasome, have important functions in eukaryotic cells to maintain proteostasis (31). In fact, MG132, a reversible peptide-aldehyde inhibitor of proteasomes, has been used extensively as a research tool to investigate the ubiquitin-proteasome system in mammalian cells and was the lead compound for the development of an anticancer agent (32). Several of these agents have undergone extensive preclinical and clinical development in regard to target specificity and tolerability for cancer indications (33, 34), which afforded us the oppor-

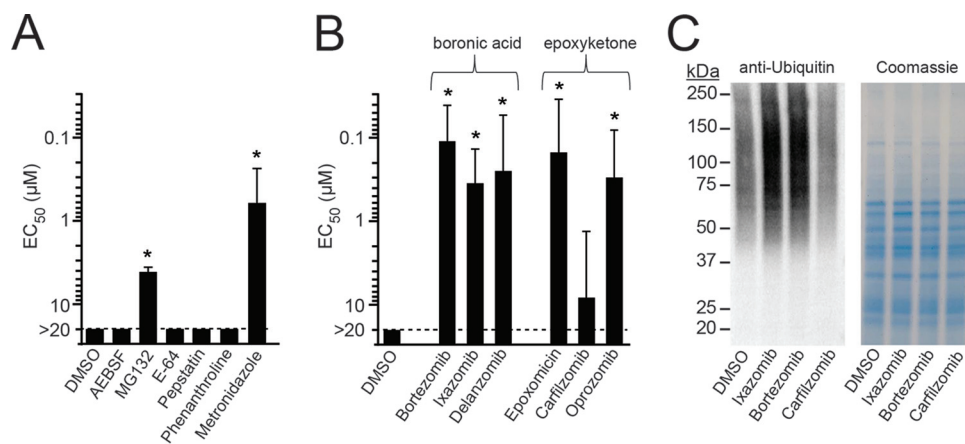


FIG 1 Trichomonacidal activity of proteasome inhibitors. (A and B) Activity of the indicated protease and proteasome inhibitors and of metronidazole as the reference drug against *T. vaginalis* F1623 trophozoites was evaluated *in vitro* in a 24-h growth and survival assay with ATP content as readout. Results are shown as the EC₅₀, the effective compound concentration that resulted in 50% inhibition of growth and survival. Data are means + standard errors of three separate experiments. **P* < 0.05, for results with the drugs versus those with the DMSO control (by analysis of variance). (C) Immunoblot analysis of ubiquitin-labeled proteins in *T. vaginalis* lysates after 1 h treatment with a 1 µM concentration of the indicated proteasome inhibitors or vehicle alone (DMSO). Total protein was analyzed by staining a parallel gel with Coomassie brilliant blue.

tunity to utilize them for further exploration of the proteasome as a new trichomonacidal target. We evaluated three covalent reversible inhibitors containing boronic acid-reactive groups and three irreversible inhibitors with epoxyketone-reactive groups (Fig. 1B). All but one of the six proteasome inhibitors displayed significant activity against *T. vaginalis* trophozoites, with EC₅₀ values that were 2- to 5-fold better than the value for the reference drug metronidazole. These initial studies showed that proteasome inhibitors with different chemically reactive warheads were effective against *T. vaginalis* with potencies that match or exceed the current standard drug.

On-target activity of proteasome inhibitors in *T. vaginalis*. In eukaryotes, proteins destined for degradation by the proteasome are first conjugated with one or more ubiquitin chains and then transported to the proteasome, where the ubiquitin chains are removed and the protein substrate is degraded. Consequently, inhibition of the proteasome leads to accumulation of ubiquitinated proteins in the cell, providing a functional readout for proteasome inhibitors (35). Therefore, we treated *T. vaginalis* with three of the proteasome inhibitors and examined the abundance of ubiquitin-labeled proteins by immunoblotting with an antibody against ubiquitin. Treatment with ixazomib and bortezomib at 1 µM (equivalent to about 2× to 5× the EC₅₀ for these agents) for 1 h led to a substantial increase in ubiquitinated proteins (Fig. 1C). In contrast, addition of carfilzomib at 1 µM, which represented only 0.1× the EC₅₀, did not alter the abundance of ubiquitin-labeled proteins compared to level with the solvent (dimethyl sulfoxide [DMSO]) control (Fig. 1C). These results indicate that ubiquitin labeling of proteins correlated with the potency of the proteasome inhibitors, suggesting that the drugs had the expected on-target activity in *T. vaginalis* even though they were not developed for this application.

Enrichment of *T. vaginalis* 20S proteasome. To further explore the biochemical specificity of the proteasome inhibitors in *T. vaginalis*, we developed a two-step fractionation protocol to enrich for the proteasome of the parasite. Cellular lysates were first fractionated by DEAE anion exchange column chromatography, and enzymatic activity in each of the eluted fractions was monitored with a standard fluorescent substrate, Suc-LLVY-AMC (succinyl-Leu-Leu-Val-Tyr-amino-4-methylcoumarin) (Fig. 2A), which detects chymotrypsin-type activity in human, *Saccharomyces cerevisiae*, parasite, and bacterial proteasomes (21, 36, 37). Fractions with the highest activity were pooled, concentrated, and further separated by gel filtration chromatography using a

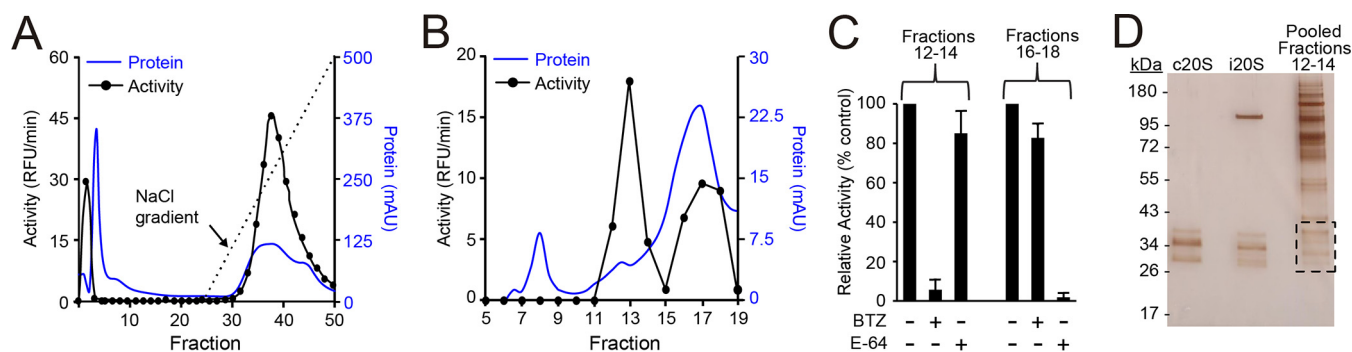


FIG 2 Enrichment of *T. vaginalis* proteasome. Total lysates of *T. vaginalis* F1623 were prepared and enriched for the 20S proteasome by two-step column chromatography. (A) Lysates were first fractionated with a DEAE anion exchange column, and fractions were eluted with a NaCl gradient and assayed for total protein (blue line) and enzymatic activity with the substrate Suc-LLVY-AMC (black line). AU, arbitrary units. (B) Fractions 33 to 37 were then pooled and further separated by gel filtration using a Superose 6 column. Fractions were again assayed for total protein (blue line) and enzymatic activity (black line). (C) Fractions 12 to 14 and 16 to 18 of the second fractionation were pooled, and the pools were tested for sensitivity to the proteasome inhibitor, bortezomib (BTZ), and the cysteine protease inhibitor, E-64. Data are expressed relative to the activity in vehicle-treated controls (means + standard errors, $n = 3$; * $P < 0.05$, for results with the inhibitors versus those with the respective vehicle controls). (D) The pool of fractions 12 to 14 and purified preparations of the human constitutive proteasome (c20S) and human immunoproteasome (i20S) were run on a denaturing SDS-PAGE gel and stained with silver. Proteins shown in the boxed area were excised and subjected to proteomic analysis.

Sepharose-6 size exclusion column. Activity assays of the eluted fractions with the same Suc-LLVY-AMC substrate yielded two well-defined activity peaks (Fig. 2B). Proteolytic activity in fractions 12 to 14 was inhibited by the proteasome inhibitor bortezomib, whereas activity in fractions 16 to 18 was insensitive to bortezomib but sensitive to the cysteine protease inhibitor E-64 (Fig. 2C). These data show that our fractionation strategy could separate the large proteasome complex of *T. vaginalis* with chymotrypsin-type activity from lower-molecular-weight cysteine proteases.

The proteins in pooled fractions 12 to 14 representing the proteasome were visualized by silver staining following denaturing gel electrophoresis. As controls, the human constitutive proteasome (c20S) and human immunoproteasome (i20S) were run in parallel. The α and β subunits of c20S and i20S migrated in the expected molecular-weight range of 22 to 38 kDa (Fig. 2D) (38). Several *T. vaginalis* proteins were visible in the same mass range although a number of higher-molecular-weight proteins were also detected (Fig. 2D). We excised the region from the *T. vaginalis* lane that corresponded in mass to the human α and β subunits and analyzed the proteins with proteomic methods. Seven putative α and β subunits were identified in the gel section, confirming that we had successfully enriched the 20S proteasome from the *T. vaginalis* (Tv20S) protein extract.

Proteasomes are structurally highly conserved, consisting of two rings of seven α and two rings of seven β subunits that assemble into a core complex of 28 proteins. The β_1 , β_2 , and β_5 subunits generally have catalytic activity, with the active sites facing the inner channel of the proteasome (Fig. 3A). In the mammalian proteasome, the three catalytic β subunits have different substrate preferences, as illustrated by the differently shaped active sites in Fig. 3A. The proteasome subunits of *T. vaginalis* are poorly annotated, so we performed protein sequence alignments with the human α and β subunits. The resulting dendrogram shows that each *T. vaginalis* subunit aligned to a single c20S subunit with between 28% and 52% sequence identity (Fig. 3B). In addition, we confirmed that the *T. vaginalis* proteins [A2E7Z2](#), [A2F2T6](#), and [A2DD57](#) (UniProt accession numbers) closely align with the human β_1 , β_2 , and β_5 subunits, respectively, and that each of these subunits contains the critical active-site triad of Thr-1, Asp-17 and Lys-33 (mature protein numbering) (Fig. 3C). Therefore, we conclude that *T. vaginalis* possesses the same three catalytically active proteasome β subunits as other eukaryotic cells.

Differential activity of ixazomib against human and *T. vaginalis* proteasome β subunits. To identify a candidate proteasome inhibitor for further biochemical studies and *in vivo* efficacy testing, we evaluated each of the proteasome inhibitors in a HeLa

Suc-LLVY-AMC. The drug was a potent inhibitor of both the human and parasite $\beta 5$ subunits, with similar 50% inhibitory concentration (IC_{50}) values (Fig. 4B). In contrast, using the $\beta 1$ substrate Z-LLE-AMC (carboxybenzyl-Leu-Leu-Gly-7-amino-4-methylcoumarin), ixazomib was found to be a weak inhibitor of the $\beta 1$ subunit of Tv20S, whereas it inhibited the human $\beta 1$ subunit as effectively as the $\beta 5$ subunit (Fig. 4C). These studies suggest that human cytotoxicity of ixazomib is associated with dual inhibition of the c20S $\beta 1$ and $\beta 5$ subunits, whereas inhibition of the $\beta 5$ subunit alone may be sufficient for trichomonad activity.

In vivo efficacy of ixazomib in a murine trichomonad infection model. To test for *in vivo* efficacy of ixazomib, we employed *T. foetus*, a trichomonad species related to *T. vaginalis* but with more robust vaginal infectivity in mice (39). We first confirmed that ixazomib was active against *T. foetus* trophozoites *in vitro* (EC_{50} of $4.3 \pm 0.3 \mu M$). Female BALB/c mice (3 to 4 weeks old) were then infected intravaginally with *T. foetus* trophozoites and subsequently treated with five intravaginal doses of ixazomib or vehicle control over a 3-day period (Fig. 4D, top). Treatment with ixazomib eradicated the parasites, whereas >85% of vehicle-treated mice had between 5×10^3 and 2×10^5 trophozoites per mouse (Fig. 4D). Furthermore, treatment with only three doses of ixazomib also led to a marked reduction in parasite numbers, indicating that fewer than five doses can be therapeutic (Fig. 4D). No apparent adverse effects were observed in any of the ixazomib-treated mice, demonstrating that proteasome inhibition is a viable therapeutic strategy against vaginal trichomonad infection and has the potential for reduced systemic adverse effects through effective topical application.

Carmaphycins as proteasome inhibitors with increased *T. vaginalis* selectivity. Although ixazomib had marked trichomonad activity *in vitro* and *in vivo*, its significant human cytotoxicity and lack of selectivity (Fig. 4A) would presumably preclude its use as an anti-infective agent. Alternative compounds with greater selectivity are likely to be needed for therapy of trichomoniasis. In previous work by our group, we isolated a compound from a marine cyanobacterium, carmaphycin B (CPB) (Fig. 5A), which displays potent inhibitory activity against human and *Plasmodium* proteasomes (40). In an effort to make a selective *Plasmodium* proteasome inhibitor with reduced mammalian cytotoxicity, we synthesized 20 derivatives of CPB with the general structure of an N-terminal hexanoic acid group, a tripeptide sequence (P3-P2-P1), and a C-terminal epoxyketone group (21) (Fig. 5A). We evaluated this targeted compound library for activity against *T. vaginalis* and HeLa cells. The parent compound, CPB, was active against *T. vaginalis*, with an EC_{50} of 490 nM, but was also highly cytotoxic in HeLa cells (50% cytotoxic concentration [CC_{50}], 5 nM) (Fig. 5B). In contrast, the derivatives showed a spectrum of activities against *T. vaginalis* and HeLa cells (Fig. 5B). For example, carmaphycin-17 (CP-17), consisting of bulky aromatic groups (indole and phenyl) in the P1, P2, and P3 positions, had 493-fold reduced HeLa cytotoxicity compared to that of CPB but a 2-fold increase in potency for *T. vaginalis* (EC_{50} of 217 nM), resulting in a dramatic 1,113-fold improvement in selectivity (Fig. 5B). On the other hand, carmaphycin-18 (CP-18), which mostly differs from CPB in the P2 and P3 positions (Fig. 5A), had no effect on *T. vaginalis* or HeLa cells at 20 μM (Fig. 5B). Consistent with the cell killing data, incubation of *T. vaginalis* with CP-17 resulted in an increase in ubiquitinated proteins similar to that found with ixazomib, whereas CP-18 had no effect (Fig. 5C).

To explore the biochemical basis of the improved selectivity of CP-17, we assayed its activity against the $\beta 1$ and $\beta 5$ subunits of Tv20S and c20S. The compound was >5-fold more active against the $\beta 5$ subunit of the parasite proteasome than that of the human proteasome (Fig. 5D). Furthermore, CP-17 was also more potent at targeting the Tv20S $\beta 1$ subunit than the human c20S equivalent (Fig. 5E) even though the potency against this subunit was much lower than that against the $\beta 5$ subunit. These results suggest that the *T. vaginalis* proteasome is functionally distinct from the human constitutive proteasome and that this difference can be exploited for the development of more selective proteasome inhibitors against the parasite.

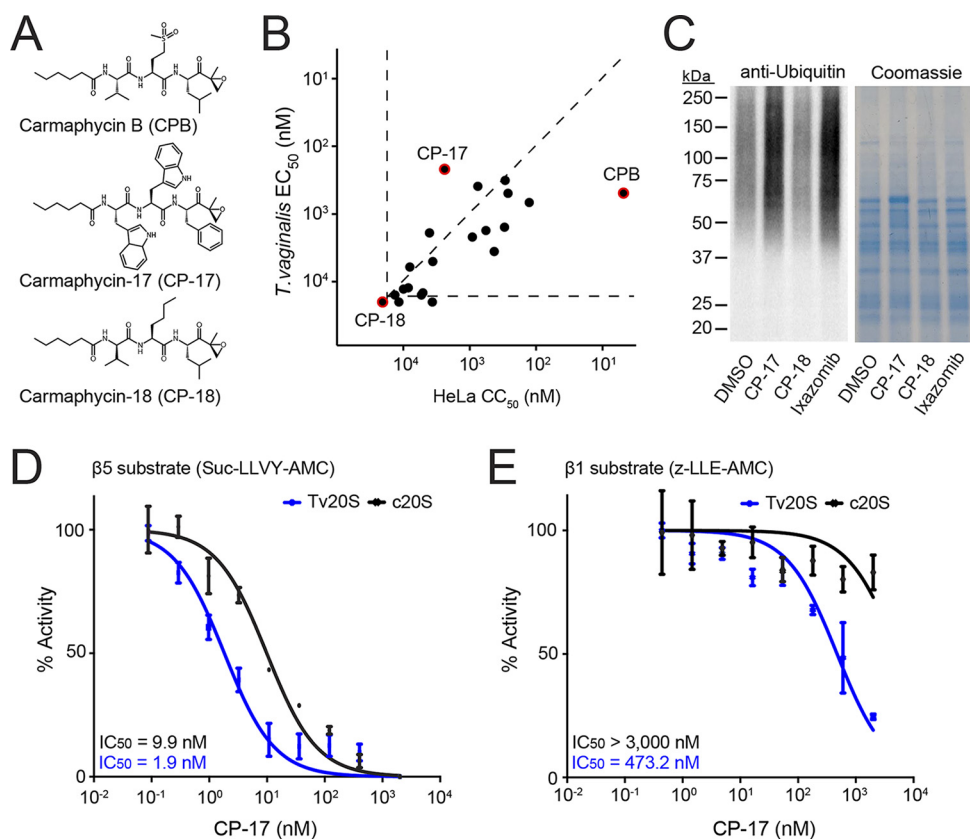


FIG 5 Carmaphycin derivatives as proteasome inhibitors with improved selectivity against *T. vaginalis*. (A) Structures of the marine natural product carmaphycin B (CPB) and two synthetic derivatives, carmaphycin-17 (CP-17) and carmaphycin-18 (CP-18). (B) A library of 20 carmaphycin derivatives was tested for activity (EC_{50}) against *T. vaginalis* and cytotoxicity (CC_{50}) against human HeLa cells. Each data point represents the mean values of EC_{50} and CC_{50} of three independent experiments; data for CPB, CP-17, and CP-18 are highlighted in red. The horizontal and vertical dashed lines represent the assay sensitivities. Compounds that had no detectable activity are shown below or to the left of these lines. For comparison, the diagonal dashed line depicts a selectivity ratio (CC_{50}/EC_{50}) of 1, so compounds located below that line are more active against human cells than against the parasite, while compounds above the line are more active against the parasite than against human cells. (C) Immunoblot analysis of ubiquitin-labeled proteins in *T. vaginalis* lysates after 1-h treatment with a 1 μ M concentration of the indicated proteasome inhibitors or vehicle alone (DMSO). Total protein was visualized by Coomassie brilliant blue staining. (D and E) CP-17 was assayed for inhibition of the β_5 subunit and β_1 subunit of the enriched Tv20S (blue lines; corresponding to fractions 12 to 14 in Fig. 2C) and purified human c20S (black lines), using subunit-specific substrates. Data are expressed relative to activity without inhibitor and are shown as means \pm standard errors ($n = 3$). Potency was calculated by extrapolation and is shown as IC_{50} , the inhibitory concentration that inhibited 50% of the enzyme activity in the assay. For c20S in panel E, none of the data points showed more than 50% inhibition, so the IC_{50} could not be calculated; instead, it is shown as exceeding the highest tested drug concentration.

Carmaphycin-17 can overcome metronidazole resistance in *T. vaginalis* and has significant *in vivo* efficacy against trichomonads.

An important rationale for developing new classes of drugs against trichomoniasis is the increasing occurrence of resistance to the most commonly used trichomonocidal drug, metronidazole (12). Therefore, we tested the activity of CP-17, as well as ixazomib, against a metronidazole-resistant strain of *T. vaginalis* (41). Both compounds were equally or even slightly more effective against the resistant line than against the susceptible strain of *T. vaginalis*, in contrast to metronidazole, which showed the expected \sim 10-fold decrease in potency against the resistant strain (Fig. 6A) (41). Furthermore, ixazomib and CP-17 showed similar potencies against a third, unrelated *T. vaginalis* strain (Fig. 6A). These data show that metronidazole resistance does not impact the activity of proteasome inhibitors against *T. vaginalis* and that such inhibitors are active against several different strains, thus underlining that these compounds represent a mechanistically novel class of trichomonocidal drugs.

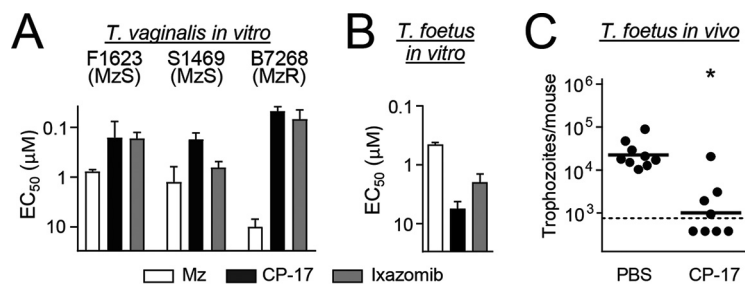


FIG 6 Activity of carmaphycin derivative against metronidazole-resistant *T. vaginalis* and vaginal trichomonad infection. (A) The proteasome inhibitors CP-17 and ixazomib (as a control) were tested for activity (EC₅₀) against metronidazole (Mz)-sensitive (MzS) and Mz-resistant (MzR) strains of *T. vaginalis* in a 24-h growth and survival assay, with ATP content as readout. Data are means + standard errors of three separate experiments. (B) CP-17 and ixazomib were also tested for activity (EC₅₀) against *T. foetus* (mean + standard error; $n = 3$). (C) *T. foetus*-infected mice were given five intravaginal treatments with a 1% (15 mM) suspension in CP-17 or PBS as outlined in the legend of Fig. 4D, and live parasites were enumerated in vaginal washes 1 day after the last treatment. Each point represents an individual mouse, and horizontal bars show geometric means (*, $P < 0.05$ for results with the drugs versus those with the controls by a Mann-Whitney U test). The dashed line shows the detection limit of the assay.

To further evaluate utility of CP-17 as a new lead compound, we investigated its *in vivo* efficacy against vaginal trichomonad infection. We first confirmed that CP-17, like ixazomib, had significant *in vitro* activity against the model parasite, *T. foetus* (Fig. 6B). Subsequently, *T. foetus*-infected mice were given five topical administrations of the compound over 3 days, and parasite numbers were evaluated in vaginal washes. CP-17 led to a significant 20-fold reduction in trophozoite numbers compared to levels for the vehicle-treated controls (Fig. 6C). None of the drug-treated mice showed any apparent adverse effects. These data demonstrate that CP-17 has significant *in vivo* efficacy against trichomonads, further supporting its potential as a promising new drug lead.

DISCUSSION

Our studies advance the *T. vaginalis* proteasome as a new target for development of potent antimicrobials against trichomoniasis. Proteasome inhibitors were lethal to the parasite *in vitro* and *in vivo*, and bioactivity was associated with engagement of the predicted drug target. Other recent reports have also validated the proteasome as a drug target for disease-causing microbes (23, 42). For example, saturation mutagenesis revealed that many essential genes of *P. falciparum* are in the proteasome degradation pathway (43), and proteasome inhibitors have shown promise as new antimalarial agents (21, 44–46). Similarly, inhibition of the proteasome in the kinetoplastid parasites, *Trypanosoma* and *Leishmania*, is toxic to the parasites *in vitro* and clears infection in murine models (23). Thus, our results and those in other parasites add to the emerging concept that the proteasome is a drug target against a wide range of eukaryotic pathogens.

Key to the development and ultimate utility of proteasome inhibitors as anti-infectives will be maximizing selectivity relative to human cells. We found that the improved selectivity of the most promising compound, CP-17, against *T. vaginalis* over human cells was paralleled by a >5-fold greater potency against the $\beta 1$ and $\beta 5$ proteasome subunits of the parasite than that against the human subunits. In contrast, another inhibitor, CP-18, which blocked the $\beta 5$ proteasome subunit in *Plasmodium falciparum* and had the best antimalarial potency and selectivity of a group of carmaphycin derivatives (21), was inactive against *T. vaginalis*. Together, these observations indicate that the proteasomes of different species have unique substrate specificities, a contention generally supported by analysis of cleavage specificities and structural modeling (36, 47–49). As a practical consequence, proteasome inhibitors developed for a particular infectious indication may not be easily repurposed for other indications, so separate medicinal chemistry efforts will probably be needed for further development of the current lead, CP-17, into an optimal trichomonacidal agent. Such development

would also have to consider optimal pharmacokinetic characteristics since CP-17 has so far proved to be less efficacious *in vivo* than ixazomib despite its slightly greater *in vitro* potency. However, our dosing experiments with ixazomib suggest that it might be possible to develop high-potency compounds that could be therapeutic with small numbers and perhaps only a single drug administration.

The mechanisms by which proteasome inhibition causes cell death in parasites are not well defined. In human cancer cells, proteasome inhibitors prevent clearance of unfolded or misfolded proteins that are cytotoxic to the cells (19). They also inhibit I κ B kinase degradation, thereby preventing the induction of gene products with pro-survival functions and leading to caspase-mediated cell death (50). In *P. falciparum*, treatment with proteasome inhibitors results in accumulation of polyubiquitinated proteins that activate an endoplasmic reticulum stress response, which ultimately leads to cell death (51). Interestingly, another antimalarial drug, dihydroartemisinin, also causes accumulation of polyubiquitinated proteins and synergizes with proteasome inhibitors to kill cells, underlining the utility of the proteasome as a drug target (52). As for *P. falciparum*, treatment of *T. vaginalis* for only 1 h with proteasome inhibitors resulted in a significant accumulation of ubiquitinated proteins, suggesting that cell death in this parasite may occur by a mechanism similar to that in *P. falciparum*. Furthermore, depending on growth conditions, inhibition of the proteasome may also induce autophagy in *T. vaginalis*, which, if excessive, could induce cell death (28).

The trichomonocidal activity of proteasome inhibitors was not impacted by resistance to the most commonly used drug for treating trichomoniasis, metronidazole. This suggests that proteasome inhibition holds promise as a rescue therapy for infections refractory to nitro drugs (11, 53). Nitro drugs act in a two-step sequence, involving initial activation by reduction to reactive intermediates, followed by covalent binding of intermediates to and inactivation of multiple target molecules. Resistance is caused by loss of the necessary reductases (9), a process that is evidently unrelated to the ubiquitin-proteasome system. This molecular target independence raises the future possibility that nitro drugs and proteasome inhibitors may exhibit synergistic activity in *T. vaginalis* killing.

Both proteasome inhibitors that were tested *in vivo*, ixazomib and CP-17, were active against vaginal trichomonad infection after topical administration, albeit with differences in their efficacies. Treatment of multiple myeloma with proteasome inhibitors is by intravenous or oral drug administration (19, 54), so a suitable drug against *T. vaginalis* may also be effective through those routes. However, topical administration has potential advantages over systemic routes, including the possibility of reduced systemic exposure and thus a lower risk of adverse effects. Although currently approved trichomonocidal drugs are only given orally, partly because of insufficient efficacy with achievable topical doses (55), other vaginal infections are treated or protected against with vaginal creams, gels, dissolvable tablets, or suppositories (56). For those drugs, tissue levels in the mid-micromolar range are achievable (57, 58), which are well above the range of potencies we found for proteasome inhibitors. It remains to be determined whether topical treatment is feasible in males infected with *T. vaginalis*, but it is noteworthy that the urgency for alternative treatment strategies is greater in females, where infection can persist for months or even years, than in males, where infection generally lasts less than 10 days (59). Overall, our findings demonstrate that proteasome inhibition is a viable new therapeutic strategy for trichomoniasis and thus, provides an impetus to the systematic development of suitable inhibitors with improved potency, selectivity, and *in vivo* efficacy.

MATERIALS AND METHODS

Drugs and chemicals. Protease inhibitors were purchased from Selleckchem (Houston, TX, USA). Carmaphycin B and analogs were synthesized as described previously (21). Human 20S constitutive proteasome, human 20S immunoproteasome, and fluorescent substrates were purchased from Boston Biochem (Cambridge, MA).

Antimicrobial and cytotoxicity assays. The following trichomonad strains were used: metronidazole-sensitive *T. vaginalis* F1623 and S1469 (60), metronidazole-resistant *T. vaginalis* B7268 (41, 61), and

metronidazole-sensitive *T. foetus* D1 (62). Cells were grown at 37°C in TYM (trypticase, yeast extract, maltose) Diamond's medium supplemented with 180 μ M ferrous ammonium sulfate. Drug susceptibility assays were done as described previously (41). Briefly, stocks of the test compounds were diluted in phosphate-buffered saline (PBS) to 75 μ M, and 1:3 serial dilutions were made. Trophozoites (3×10^3 /well) were added to 96-well plates, and cultures were incubated for 24 h at 37°C under anaerobic conditions (AnaeroPack-Anaero system). Growth and viability were determined with an ATP assay by adding BacTiter-Glo microbial cell viability assay reagent (Promega) and measuring ATP-dependent luminescence in a microplate reader. The 50% effective concentration (EC_{50}) was derived from the concentration-response curves using BioAssay software (CambridgeSoft Software).

Proteasome enrichment. *T. vaginalis* lysates were prepared in a buffer of 100 mM NaCl, 20 mM Tris (pH 7.5), 0.01% Tween 20, 0.5% glycerol, and 100 μ M E-64 by sonication for 30 s and three subsequent freeze-thaw cycles. Protein amounts were determined by bicinchoninic acid assay. Tv20S was enriched from the lysates by two chromatographic steps. In a first enrichment step, lysate (~8.5 mg of protein in 2 ml) was loaded onto a 5-ml anion exchange HiTrap DEAE FF column (GE Healthcare) connected to an AKTA Pure instrument (GE Healthcare). Unbound proteins were removed by washing with a buffer of 25 mM Tris (pH 7.5), 1 mM dithiothreitol (DTT), and 10% glycerol. Bound proteins were eluted with 25 ml of a linear gradient from 0 to 0.5 M NaCl, with collection of 1.5-ml fractions. Aliquots of the fractions were analyzed for proteasome activity with a 25 μ M concentration of the substrate succinyl-Leu-Leu-Val-Tyr-7-amino-4-methylcoumarin (Suc-LLVY-AMC) in a buffer of 20 mM Tris (pH 7.5), 10 mM $MgCl_2$, 1 mM DTT, 1 mM ATP, and 0.02% SDS, with and without 10 μ M bortezomib or 10 μ M E-64. Fractions containing bortezomib-sensitive activity were pooled and concentrated to 0.5 ml using a 100-kDa centrifugal filter (Amicon). In a second step, pooled fractions were loaded onto a Superose 6 10/300 gel filtration column (GE Healthcare). Proteins were eluted with 1.5 column volumes of 25 mM Tris (pH 7.5), 1 mM DTT, 10% glycerol, and 125 mM NaCl into 1-ml fractions, which were assayed again for proteolytic activity with Suc-LLVY-AMC, with and without 10 μ M bortezomib or 10 μ M E-64. Bortezomib-sensitive fractions without detectable E-64 sensitive activity (fractions 12 to 14) (Fig. 2C) were pooled and used for all biochemical and structural characterization of Tv20S.

Proteomics. Tv20S was analyzed by electrophoresis together with 100 ng of c20S and i20S. Samples were treated with NuPAGE lithium dodecyl sulfate (LDS) sample buffer (Thermo Fisher Scientific), denatured at 85°C for 10 min, run on a 4 to 12% Bis-Tris Plus gel (Thermo Fisher Scientific), and stained with silver. The appropriate bands were excised from the gel with a clean scalpel, diced into 1-mm cubes, and placed into 0.6-ml tubes (Axygen). In-gel trypsin digestion was performed as described previously (63). Following digestion and extraction, the peptides were desalted with C_{18} LTS tips (Rainin) and dried in a vacuum centrifuge. Peptides were resuspended in 12 μ l of 0.1% trifluoroacetic acid (TFA), and 5 μ l was analyzed on a Q Exactive mass spectrometer (MS) (Thermo Scientific). Peptides were first separated by reverse-phase chromatography on an UltiMate 3000 high-performance liquid chromatography (HPLC) system (Thermo Scientific) equipped with an in-house packed C_{18} column (1.7- μ m bead size, 75 μ m by 25 cm, heated to 65°C) at a flow rate of 300 nl/min over a 76-min linear gradient from 5% solvent A to 25% solvent B, where solvent A and B correspond to 0.1% formic acid in water and 0.1% formic acid in acetonitrile, respectively. Survey scans were recorded at a resolution of 35,000 at 200 m/z over a range of 350 to 1,500 m/z with the automatic gain control (AGC) at 1×10^6 and a maximum injection time of 300 ms. Tandem MS (MS/MS) was performed in data-dependent acquisition mode with higher-energy collision dissociation fragmentation (28 normalized collision energy) on the 20 most intense precursor ions at a resolution of 17,500 at 200 m/z , with the AGC at 5×10^6 and a maximum injection time of 50 ms.

Data analysis was performed using the PEAKS, version 8.5, software (Bioinformatics Solutions, Inc.). RAW files were searched against the reference proteome of *T. vaginalis* strain ATCC PRA-98 from UniProt (<https://www.uniprot.org/proteomes/UP000001542>) with 50,190 entries using the following settings: 15 ppm precursor mass tolerance, 0.01 Da MS/MS mass tolerance, and an enzyme digest of trypsin with a maximum of three missed cleavages. Carbamidomethylation of cysteines was included as a fixed modification, and oxidation of methionine and protein N-terminal acetylation were included as variable modifications. The false discovery rate for protein identification was set to 1%. Annotation of the putative *T. vaginalis* proteasome subunits with α and β subunit nomenclature was performed by comparing sequence alignments against the human 20S proteasome subunits with BLAST, version 2.6.0+, command line tools.

Proteasome assays. Proteasome activity was assayed using 0.29 nM c20S or Tv20S in 20 mM Tris (pH 7.5), 10 mM $MgCl_2$, 1 mM DTT, 1 mM ATP, 0.02% SDS, and 25 μ M Suc-LLVY-AMC or 25 μ M carboxybenzyl-Leu-Leu-Gly-7-amino-4-methylcoumarin (Z-LLE-AMC) in 50- μ l reaction mixtures in black-walled 96-well plates. AMC fluorophore release was monitored at excitation 360 nm and emission 460 nm at 24°C using a Synergy HTX multimode reader (Biotek). For inhibition assays, substrate and inhibitor were added simultaneously to the enzyme, and the reaction rate, expressed in relative fluorescence units (RFU) per second, was determined for 4 h. The 50% inhibitory concentration (IC_{50}) was calculated in GraphPad Prism, version 6, by normalizing activity to that of the DMSO controls and interpolating the data using the log(inhibitor)-variable slope curve fitting algorithm.

Immunoblot analysis. *T. vaginalis* F1623 was incubated for 1 h with 1 μ M proteasome inhibitor or solvent control, and cells were lysed using radioimmunoprecipitation assay (RIPA) buffer with added Halt protease inhibitors (Thermo Scientific). Protein concentrations were measured with detergent-compatible (DC) protein assay (Bio-Rad) and adjusted to 10 mg/ml. Proteins were fractionated by SDS-PAGE, transferred onto a nitrocellulose membrane (Bio-Rad), which was blocked with 5% nonfat dry milk in TBST buffer (20 mM Tris base, 150 mM NaCl, 0.05% Tween 20, pH adjusted to 7.6 with HCl) for 1 h, and probed with primary anti-ubiquitin K48 antibody (Boston Biochem) at a 1:5,000 dilution, followed

by incubation with anti-rabbit horseradish peroxidase (HRP)-conjugated IgG (Jackson laboratory) at a 1:10,000 dilution. Immunoreactions were visualized by chemiluminescence (Immobilon, Millipore).

Murine trichomonad infection model. Weanling (3- to 4-week-old) female BALB/CJ mice were inoculated intravaginally with 5 μ l of a suspension containing 10⁶ *T. foetus* D1 trophozoites in TYM medium. For drug treatment studies, mice were given 5 μ l/dose of 0.5% (14 mM) ixazomib or 1% (15 mM) of CP-17 in 0.1% hypromellose (Sigma), or vehicle controls, intravaginally five or three times for 3 days beginning 1 day after infection. On day 4, live trophozoites were enumerated in vaginal washes. All animal studies were reviewed and approved by the Institutional Animal Care and Use Committee of the University of California, San Diego.

Data availability. The complete mass spectrometry data and annotations can be accessed on the Mass Spectrometry Interactive Virtual Environment (MassIVE) public data repository under accession number MSV000083474. The FTP download link is <ftp://massive.ucsd.edu/MSV000083474>.

ACKNOWLEDGMENTS

This work was supported by NIH grants AI146387 (A.J.O. and L.E.), AI133393 (A.J.O. and C.R.C.), CA100851 (W.H.G.), AI114671 (L.E.), and DK120515 (L.E.) and a UCSD Academic Senate Research Grant (A.J.O. and C.R.C.). Z.J. is supported by the UCSD Chancellor's Research Excellence Scholarship. J.A. is grateful to the University of Jordan and the Scientific Research Support Fund for financial support. The funders had no role in study design, data collection and interpretation, or the decision to submit the work for publication.

We thank Elaine Hanson and Lucia Hall for expert technical support.

REFERENCES

- Newman L, Rowley J, Vander Hoorn S, Wijesooriya NS, Unemo M, Low N, Stevens G, Gottlieb S, Kiarie J, Temmerman M. 2015. Global estimates of the prevalence and incidence of four curable sexually transmitted infections in 2012 based on systematic review and global reporting. *PLoS One* 10:e0143304. <https://doi.org/10.1371/journal.pone.0143304>.
- Menezes CB, Frasson AP, Tasca T. 2016. Trichomoniasis—are we giving the deserved attention to the most common non-viral sexually transmitted disease worldwide? *Microb Cell* 3:404–419. <https://doi.org/10.15698/mic2016.09.526>.
- Poole DN, McClelland RS. 2013. Global epidemiology of *Trichomonas vaginalis*. *Sex Transm Infect* 89:418–422. <https://doi.org/10.1136/sextrans-2013-051075>.
- Patel EU, Gaydos CA, Packman ZR, Quinn TC, Tobian A. 2018. Prevalence and correlates of *Trichomonas vaginalis* infection among men and women in the United States. *Clin Infect Dis* 67:211–217. <https://doi.org/10.1093/cid/ciy079>.
- Swygard H, Sena AC, Hobbs MM, Cohen MS. 2004. Trichomoniasis: clinical manifestations, diagnosis and management. *Sex Transm Infect* 80:91–95. <https://doi.org/10.1136/sti.2003.005124>.
- Fichorova RN. 2009. Impact of *T. vaginalis* infection on innate immune responses and reproductive outcome. *J Reprod Immunol* 83:185–189. <https://doi.org/10.1016/j.jri.2009.08.007>.
- McClelland RS, Sangare L, Hassan WM, Lavreys L, Mandaliya K, Kiarie J, Ndinya-Achola J, Jaoko W, Baeten JM. 2007. Infection with *Trichomonas vaginalis* increases the risk of HIV-1 acquisition. *J Infect Dis* 195:698–702. <https://doi.org/10.1086/511278>.
- Marous M, Huang WY, Rabkin CS, Hayes RB, Alderete JF, Rosner B, Grubb RL, III, Winter AC, Sutcliffe S. 2017. *Trichomonas vaginalis* infection and risk of prostate cancer: associations by disease aggressiveness and race/ethnicity in the PLCO Trial. *Cancer Causes Control* 28:889–898. <https://doi.org/10.1007/s10552-017-0919-6>.
- Uprocroft P, Uprocroft JA. 2001. Drug targets and mechanisms of resistance in the anaerobic protozoa. *Clin Microbiol Rev* 14:150–164. <https://doi.org/10.1128/CMR.14.1.150-164.2001>.
- Uprocroft JA, Dunn LA, Wal T, Tabrizi S, Delgado-Correa MG, Johnson PJ, Garland S, Siba P, Uprocroft P. 2009. Metronidazole resistance in *Trichomonas vaginalis* from highland women in Papua New Guinea. *Sex Health* 6:334–338. <https://doi.org/10.1071/SH09011>.
- Cudmore SL, Delgaty KL, Hayward-McClelland SF, Petrin DP, Garber GE. 2004. Treatment of infections caused by metronidazole-resistant *Trichomonas vaginalis*. *Clin Microbiol Rev* 17:783–793. <https://doi.org/10.1128/CMR.17.4.783-793.2004>.
- Kirkcaldy RD, Augostini P, Asbel LE, Bernstein KT, Kerani RP, Mettenbrink CJ, Pathela P, Schwabke JR, Secor WE, Workowski KA, Davis D, Braxton J, Weinstock HS. 2012. *Trichomonas vaginalis* antimicrobial drug resistance in 6 US cities, STD Surveillance Network, 2009–2010. *Emerg Infect Dis* 18:939–943. <https://doi.org/10.3201/eid1806.111590>.
- Sobel JD, Nyirjesy P, Brown W. 2001. Tinidazole therapy for metronidazole-resistant vaginal trichomoniasis. *Clin Infect Dis* 33:1341–1346. <https://doi.org/10.1086/323034>.
- Snipes LJ, Gamard PM, Narcisi EM, Beard CB, Lehmann T, Secor WE. 2000. Molecular epidemiology of metronidazole resistance in a population of *Trichomonas vaginalis* clinical isolates. *J Clin Microbiol* 38:3004–3009.
- De Ambrogi M. 2017. Turning the spotlight on sexually transmitted infections. *Lancet Infect Dis* 17:792–793. [https://doi.org/10.1016/S1473-3099\(17\)30363-8](https://doi.org/10.1016/S1473-3099(17)30363-8).
- Klausner JD, Broutet N. 2017. Health systems and the new strategy against sexually transmitted infections. *Lancet Infect Dis* 17:797–798. [https://doi.org/10.1016/S1473-3099\(17\)30361-4](https://doi.org/10.1016/S1473-3099(17)30361-4).
- Huber EM, Basler M, Schwab R, Heinemeyer W, Kirk CJ, Groettrup M, Groll M. 2012. Immuno- and constitutive proteasome crystal structures reveal differences in substrate and inhibitor specificity. *Cell* 148:727–738. <https://doi.org/10.1016/j.cell.2011.12.030>.
- Bibo-Verdugo B, Jiang Z, Caffrey CR, O'Donoghue AJ. 2017. Targeting proteasomes in infectious organisms to combat disease. *FEBS J* 284:1503–1517. <https://doi.org/10.1111/febs.14029>.
- Manasanch EE, Orłowski RZ. 2017. Proteasome inhibitors in cancer therapy. *Nat Rev Clin Oncol* 14:417–433. <https://doi.org/10.1038/nrclinonc.2016.206>.
- Li H, O'Donoghue AJ, van der Linden WA, Xie SC, Yoo E, Foe IT, Tilley L, Craik CS, da Fonseca PC, Bogoyo M. 2016. Structure- and function-based design of Plasmodium-selective proteasome inhibitors. *Nature* 530:233–236. <https://doi.org/10.1038/nature16936>.
- LaMonte GM, Almaliti J, Bibo-Verdugo B, Keller L, Zou BY, Yang J, Antonova-Koch Y, Orjuela-Sanchez P, Boyle CA, Vigil E, Wang L, Goldgof GM, Gerwick L, O'Donoghue AJ, Winzler EA, Gerwick WH, Otilie S. 2017. Development of a potent inhibitor of the Plasmodium proteasome with reduced mammalian toxicity. *J Med Chem* 60:6721–6732. <https://doi.org/10.1021/acs.jmedchem.7b00671>.
- Kirkman LA, Zhan W, Visone J, Dziedzic A, Singh PK, Fan H, Tong X, Bruzual I, Hara R, Kawasaki M, Imaeda T, Okamoto R, Sato K, Michino M, Alvaro EF, Guiang LF, Sanz L, Mota DJ, Govindasamy K, Wang R, Ling Y, Tumwebaze PK, Sukenick G, Shi L, Vendome J, Bhanot P, Rosenthal PJ, Aso K, Foley MA, Cooper RA, Kafsack B, Doggett JS, Nathan CF, Lin G. 2018. Antimalarial proteasome inhibitor reveals collateral sensitivity from inter-subunit interactions and fitness cost of resistance. *Proc Natl Acad Sci U S A* 115:E6863–E6870. <https://doi.org/10.1073/pnas.1806109115>.
- Khare S, Nagle AS, Biggart A, Lai YH, Liang F, Davis LC, Barnes SW,

- Mathison CJ, Myburgh E, Gao MY, Gillespie JR, Liu X, Tan JL, Stinson M, Rivera IC, Ballard J, Yeh V, Groessl T, Federe G, Koh HX, Venable JD, Bursulaya B, Shapiro M, Mishra PK, Spraggon G, Brock A, Mottram JC, Buckner FS, Rao SP, Wen BG, Walker JR, Tuntland T, Molteni V, Glynne RJ, Supek F. 2016. Proteasome inhibition for treatment of leishmaniasis, Chagas disease and sleeping sickness. *Nature* 537:229–233. <https://doi.org/10.1038/nature19339>.
24. Jalovecka M, Hartmann D, Miyamoto Y, Eckmann L, Hajdusek O, O'Donoghue AJ, Sojka D. 2018. Validation of Babesia proteasome as a drug target. *Int J Parasitol Drugs Drug Resist* 8:394–402. <https://doi.org/10.1016/j.ijpddr.2018.08.001>.
25. Bozner P, Demes P. 1991. Proteinases in *Trichomonas vaginalis* and *Trichomonas mobilensis* are not exclusively of cysteine type. *Parasitology* 102:113–115. <https://doi.org/10.1017/S0031182000060418>.
26. Arroyo R, Cárdenas-Guerra RE, Figueroa-Angulo EE, Puente-Rivera J, Zamudio-Prieto O, Ortega-López J. 2015. *Trichomonas vaginalis* cysteine proteinases: iron response in gene expression and proteolytic activity. *Biomed Res Int* 2015:946787. <https://doi.org/10.1155/2015/946787>.
27. Mancilla-Olea MI, Ortega-López J, Figueroa-Angulo EE, Avila-González L, Cárdenas-Guerra RE, Miranda-Ozuna JFT, González-Robles A, Hernández-García MS, Sánchez-Ayala L, Arroyo R. 2018. *Trichomonas vaginalis* cathepsin D-like aspartic proteinase (Tv-CatD) is positively regulated by glucose and degrades human hemoglobin. *Int J Biochem Cell Biol* 97:1–15. <https://doi.org/10.1016/j.biocel.2018.01.015>.
28. Huang KY, Chen RM, Lin HC, Cheng WH, Lin HA, Lin WN, Huang PJ, Chiu CH, Tang P. 2018. Potential role of autophagy in proteolysis in *Trichomonas vaginalis*. *J Microbiol Immunol Infect* <https://doi.org/10.1016/j.jmii.2018.11.002>.
29. Pereira-Neves A, Gonzaga L, Menna-Barreto RF, Benchimol M. 2015. Characterisation of 20S proteasome in *Trichomonas foetus* and its role during the cell cycle and transformation into endoflagellar form. *PLoS One* 10:e0129165. <https://doi.org/10.1371/journal.pone.0129165>.
30. Carlton JM, Hirt RP, Silva JC, Delcher AL, Schatz M, Zhao Q, Wortman JR, Bidwell SL, Alsmark UC, Besteiro S, Sicheritz-Ponten T, Noel CJ, Dacks JB, Foster PG, Simillion C, Van de Peer Y, Miranda-Saavedra D, Barton GJ, Westrop GD, Muller S, Dessi D, Fiori PL, Ren Q, Paulsen I, Zhang H, Bastida-Corcuera FD, Simoes-Barbosa A, Brown MT, Hayes RD, Mukherjee M, Okumura CY, Schneider R, Smith AJ, Vanacova S, Villalvazo M, Haas BJ, Perteu M, Feldblyum TV, Utterback TR, Shu CL, Osoegawa K, de Jong PJ, Hrđy I, Horvathova L, Zubacova Z, Dolezal P, Malik SB, Logsdon JM, Jr, Henze K, Gupta A, et al. 2007. Draft genome sequence of the sexually transmitted pathogen *Trichomonas vaginalis*. *Science* 315:207–212. <https://doi.org/10.1126/science.1132894>.
31. Mishra R, Upadhyay A, Prajapati VK, Mishra A. 2018. Proteasome-mediated proteostasis: novel medicinal and pharmacological strategies for diseases. *Med Res Rev* 38:1916–1973. <https://doi.org/10.1002/med.21502>.
32. Goldberg AL. 2012. Development of proteasome inhibitors as research tools and cancer drugs. *J Cell Biol* 199:583–588. <https://doi.org/10.1083/jcb.201210077>.
33. Vogl DT, Martin TG, Vij R, Hari P, Mikhael JR, Siegel D, Wu KL, Delforge M, Gasparetto C. 2017. Phase I/II study of the novel proteasome inhibitor delanzomib (CEP-18770) for relapsed and refractory multiple myeloma. *Leuk Lymphoma* 58:1872–1879. <https://doi.org/10.1080/10428194.2016.1263842>.
34. Kuhn DJ, Chen Q, Voorhees PM, Strader JS, Shenk KD, Sun CM, Demo SD, Bennett MK, van Leeuwen FW, Chanan-Khan AA, Orlowski RZ. 2007. Potent activity of carfilzomib, a novel, irreversible inhibitor of the ubiquitin-proteasome pathway, against preclinical models of multiple myeloma. *Blood* 110:3281–3290. <https://doi.org/10.1182/blood-2007-01-065888>.
35. Demo SD, Kirk CJ, Aujay MA, Buchholz TJ, Dajee M, Ho MN, Jiang J, Laidig GJ, Lewis ER, Parlati F, Shenk KD, Smyth MS, Sun CM, Vallone MK, Woo TM, Molineaux CJ, Bennett MK. 2007. Antitumor activity of PR-171, a novel irreversible inhibitor of the proteasome. *Cancer Res* 67:6383–6391. <https://doi.org/10.1158/0008-5472.CAN-06-4086>.
36. Luan B, Huang X, Wu J, Mei Z, Wang Y, Xue X, Yan C, Wang J, Finley DJ, Shi Y, Wang F. 2016. Structure of an endogenous yeast 26S proteasome reveals two major conformational states. *Proc Natl Acad Sci U S A* 113:2642–2647. <https://doi.org/10.1073/pnas.1601561113>.
37. Lin G, Li D, de Carvalho LP, Deng H, Tao H, Vogt G, Wu K, Schneider J, Chidawanyika T, Warren JD, Li H, Nathan C. 2009. Inhibitors selective for mycobacterial versus human proteasomes. *Nature* 461:621–626. <https://doi.org/10.1038/nature08357>.
38. Schrader J, Henneberg F, Mata RA, Tittmann K, Schneider TR, Stark H, Bourenkov G, Chari A. 2016. The inhibition mechanism of human 20S proteasomes enables next-generation inhibitor design. *Science* 353:594–598. <https://doi.org/10.1126/science.aaf8993>.
39. Cobo ER, Eckmann L, Corbeil LB. 2011. Murine models of vaginal trichomonad infections. *Am J Trop Med Hyg* 85:667–673. <https://doi.org/10.4269/ajtmh.2011.11-0123>.
40. Pereira AR, Kale AJ, Fenley AT, Byrum T, Debonsi HM, Gilson MK, Valeriote FA, Moore BS, Gerwick WH. 2012. The carmaphyicins: new proteasome inhibitors exhibiting an α,β -epoxyketone warhead from a marine cyanobacterium. *Chembiochem* 13:810–817. <https://doi.org/10.1002/cbic.201200007>.
41. Miyamoto Y, Kalisiak J, Korthals K, Lauwaet T, Cheung DY, Lozano R, Cobo ER, Upcroft P, Upcroft JA, Berg DE, Gillin FD, Fokin VV, Sharpless KB, Eckmann L. 2013. Expanded therapeutic potential in activity space of next-generation 5-nitroimidazole antimicrobials with broad structural diversity. *Proc Natl Acad Sci U S A* 110:17564–17569. <https://doi.org/10.1073/pnas.1302664110>.
42. Totaro KA, Barthelme D, Simpson PT, Jiang X, Lin G, Nathan CF, Sauer RT, Sello JK. 2017. Rational design of selective and bioactive inhibitors of the Mycobacterium tuberculosis proteasome. *ACS Infect Dis* 3:176–181. <https://doi.org/10.1021/acscinfdis.6b00172>.
43. Zhang M, Wang C, Otto TD, Oberstaller J, Liao X, Adapa SR, Udenze K, Bronner IF, Casandra D, Mayho M, Brown J, Li S, Swanson J, Rayner JC, Jiang RHY, Adams JH. 2018. Uncovering the essential genes of the human malaria parasite *Plasmodium falciparum* by saturation mutagenesis. *Science* 360:eaa97847. <https://doi.org/10.1126/science.aap7847>.
44. Xie SC, Gillett DL, Spillman NJ, Tsu C, Luth MR, Otilie S, Duffy S, Gould AE, Hales P, Seager BA, Charron CL, Bruzzese F, Yang X, Zhao X, Huang SC, Hutton CA, Burrows JN, Winzeler EA, Avery VM, Dick LR, Tilley L. 2018. Target validation and identification of novel boronate inhibitors of the *Plasmodium falciparum* proteasome. *J Med Chem* 61:10053–10066. <https://doi.org/10.1021/acs.jmedchem.8b01161>.
45. Yoo E, Stokes BH, de Jong H, Vanaerschot M, Kumar T, Lawrence N, Njoroge M, Garcia A, Van der Westhuyzen R, Momper JD, Ng CL, Fidock DA, Bogoy M. 2018. Defining the determinants of specificity of Plasmodium proteasome inhibitors. *J Am Chem Soc* 140:11424–11437. <https://doi.org/10.1021/jacs.8b06656>.
46. Li H, Ponder EL, Verdoes M, Asbjornsdottir KH, Deu E, Edgington LE, Lee JT, Kirk CJ, Demo SD, Williamson KC, Bogoy M. 2012. Validation of the proteasome as a therapeutic target in Plasmodium using an epoxyketone inhibitor with parasite-specific toxicity. *Chem Biol* 19:1535–1545. <https://doi.org/10.1016/j.chembiol.2012.09.019>.
47. Winter MB, La Greca F, Arastu-Kapur S, Caiazza F, Cimermancic P, Buchholz TJ, Anderl JL, Ravalin M, Bohn MF, Sali A, O'Donoghue AJ, Craik CS. 2017. Immunoproteasome functions explained by divergence in cleavage specificity and regulation. *Elife* 6. <https://doi.org/10.7554/eLife.27364>.
48. Huber EM, de Bruin G, Heinemeyer W, Paniagua Soriano G, Overkleef HS, Groll M. 2015. Systematic analyses of substrate preferences of 20S proteasomes using peptidic epoxyketone inhibitors. *J Am Chem Soc* 137:7835–7842. <https://doi.org/10.1021/jacs.5b03688>.
49. Lei B, Abdul Hameed MD, Hamza A, Wehenkel M, Muzyka JL, Yao XJ, Kim KB, Zhan CG. 2010. Molecular basis of the selectivity of the immunoproteasome catalytic subunit LMP2-specific inhibitor revealed by molecular modeling and dynamics simulations. *J Phys Chem B* 114:12333–12339. <https://doi.org/10.1021/jp1058098>.
50. Palombella VJ, Rando OJ, Goldberg AL, Maniatis T. 1994. The ubiquitin-proteasome pathway is required for processing the NF-kappa B1 precursor protein and the activation of NF-kappa B. *Cell* 78:773–785. [https://doi.org/10.1016/s0092-8674\(94\)90482-0](https://doi.org/10.1016/s0092-8674(94)90482-0).
51. Bridgford JL, Xie SC, Cobbold SA, Pasaje CFA, Herrmann S, Yang T, Gillett DL, Dick LR, Ralph SA, Dogovski C, Spillman NJ, Tilley L. 2018. Artemisinin kills malaria parasites by damaging proteins and inhibiting the proteasome. *Nat Commun* 9:3801. <https://doi.org/10.1038/s41467-018-06221-1>.
52. Dogovski C, Xie SC, Burgio G, Bridgford J, Mok S, McCaw JM, Chotivanich K, Kenny S, Gnadin N, Straimer J, Bozdech Z, Fidock DA, Simpson JA, Dondorp AM, Foote S, Klonis N, Tilley L. 2015. Targeting the cell stress response of *Plasmodium falciparum* to overcome artemisinin resistance. *PLoS Biol* 13:e1002132. <https://doi.org/10.1371/journal.pbio.1002132>.
53. Kung E, Furnkranz U, Walochnik J. 2019. Chemotherapeutic options for the treatment of human trichomoniasis. *Int J Antimicrob Agents* 53:116–127. <https://doi.org/10.1016/j.ijantimicag.2018.10.016>.
54. Gupta N, Hanley MJ, Xia C, Labotka R, Harvey RD, Venkatakrishnan K.

2018. Clinical Pharmacology of ixazomib: the first oral proteasome inhibitor. *Clin Pharmacokinet* <https://doi.org/10.1007/s40262-018-0702-1>.
55. duBouchet L, McGregor JA, Ismail M, McCormack WM. 1998. A pilot study of metronidazole vaginal gel versus oral metronidazole for the treatment of *Trichomonas vaginalis* vaginitis. *Sex Transm Dis* 25: 176–179. <https://doi.org/10.1097/00007435-199803000-00012>.
56. Baloglu E, Senyigit ZA, Karavana SY, Bernkop-Schnürch A. 2009. Strategies to prolong the intravaginal residence time of drug delivery systems. *J Pharm Sci* 12:312–336.
57. Srinivasan P, Zhang J, Martin A, Kelley K, McNicholl JM, Buckheit RW, Jr, Smith JM, Ham AS. 2016. Safety and pharmacokinetics of quick-dissolving polymeric vaginal films delivering the antiretroviral IQP-0528 for preexposure prophylaxis. *Antimicrob Agents Chemother* 60: 4140–4150. <https://doi.org/10.1128/AAC.00082-16>.
58. Mashingaidze F, Choonara YE, Kumar P, Du Toit LC, Maharaj V, Buchmann E, Pillay V. 2017. Submicron matrices embedded in a polymeric caplet for extended intravaginal delivery of zidovudine. *AAPS J* 19: 1745–1759. <https://doi.org/10.1208/s12248-017-0130-4>.
59. Kissinger P. 2015. Epidemiology and treatment of trichomoniasis. *Curr Infect Dis Rep* 17:484. <https://doi.org/10.1007/s11908-015-0484-7>.
60. Brown DM, Upcroft JA, Dodd HN, Chen N, Upcroft P. 1999. Alternative 2-keto acid oxidoreductase activities in *Trichomonas vaginalis*. *Mol Biochem Parasitol* 98:203–214. [https://doi.org/10.1016/s0166-6851\(98\)00169-8](https://doi.org/10.1016/s0166-6851(98)00169-8).
61. Upcroft JA, Upcroft P. 2001. Drug susceptibility testing of anaerobic protozoa. *Antimicrob Agents Chemother* 45:1810–1814. <https://doi.org/10.1128/AAC.45.6.1810-1814.2001>.
62. Skirrow SZ, BonDurant RH. 1990. Induced *Trichomonas foetus* infection in beef heifers. *J Am Vet Med Assoc* 196:885–889.
63. Shevchenko A, Tomas H, Havli J, Olsen JV, Mann M. 2006. In-gel digestion for mass spectrometric characterization of proteins and proteomes. *Nat Protoc* 1:2856–2860. <https://doi.org/10.1038/nprot.2006.468>.